*Journal of Structural Geology*, Vol. 10, No. 6, pp. 593 to 605, 1988
Printed in Great Britain

0191–8141/88 $03.00 + 0.00


# Progress in the study and modelling of similar fold interferences

M. PERRIN

Laboratoire de Géologie, Ecole des Mines de St Etienne (EMSE),
158 Cours Fauriel, 42023 Saint Etienne, France

P. H. OLTRA

Laboratoire de Géologie Dynamique, Université St Jérôme, 13397 Marseille Cédex 4, France

and

S. COQUILLART

Equipe de Communication Visuelle, Département Informatique, EMSE,
158 Cours Fauriel, 42023 Saint Etienne, France

(*Received* 3 *June* 1987; *accepted in revised form* 14 *April* 1988)

**Abstract**—Similar fold interferences are examined in two different ways.

(1) We show the importance of taking into account the original position of the stratification with respect to the orientations of two interfering fold phases. Basin and dome cases correspond to particular orientations of the interfering phases with respect to each other. In all other cases, coaxiality may be achieved for particular positions of the original stratification.

(2) We have achieved a computer-aided modelling which allows the visualization by means of sections and block-diagrams of any two or three similar fold interferences. The program allows us to define the stratification, orientations of the various phases and their profiles (sinusoidal or drawn by hand), and orientations and dimensions of the selected section or block diagram. Faults may also be represented.

This modelling method is a powerful research tool that we hope to apply in future to detailed studies of fold interferences, to achieve quantitative field models of multiply folded and faulted terranes.

## INTRODUCTION

SIMILAR folds have been defined as important geological features by various authors (Knopf & Ingerson 1938, Turner 1948, Carey 1954, 1962, Ramsay 1962b). Interference patterns of similar fold phases are commonly observed in hand samples and in the field at various scales. Two similar fold interferences have been the subject of numerous studies (Weiss 1959, Whitten 1959, Carey 1962, Ramsay 1962a, 1967, Turner & Weiss 1963). A well-known geometrical classification has been defined by Ramsay (1962a, 1967) and refined by Thiessen & Means (1980) for the case of sinusoidal fold profiles. These authors have distinguished four types of interferences: sinusoidal (Type 0), basin and dome (Type 1), coaxial (Type 3) and crescent (Type 2), the first three corresponding to particular orientations of the fold episodes. Characteristic patterns are associated with each of these types (Thiessen 1986). These results are helpful to classify natural interference patterns. However they do not allow a complete interpretation since the authors generally assumed that the originally plane layers were perpendicular to the axial plane of the first fold phase. This is a very particular case and we will show that the type of interference produced depends on the original position of the layers with respect to the orientations of the fold phases.

Geometrical modelling of two similar fold interferences was first undertaken by O'Driscoll (1962) with the help of card decks and more recently by Thiessen & Means (1980), Thiessen (1986) and Charlesworth & McLellan (1986) through computer simulation. The program presented by Charlesworth & McLellan appears to be rather limited since the interferences produced correspond to very particular cases (the axes of the two interfering folds are perpendicular and the result depends only on the dip of first fold axial plane). On the contrary, Thiessen's REFOLD program is rather promising since it "allows for the construction of multiple generations of folds of any orientation, waveform and amplitude, as well as pure shear, simple shear and faulting" (Thiessen 1986). Unfortunately the author does not give any particulars about his program and the results presented only concern interferences of two similar fold phases whose profiles are sinusoids of fixed wavelengths and amplitudes.

Stimulated by Thiessen's & Means' results, we have tried to make further progress in the understanding of similar folds and interferences and to produce, with the help of an HP 9000 computer, a general 3D geometrical

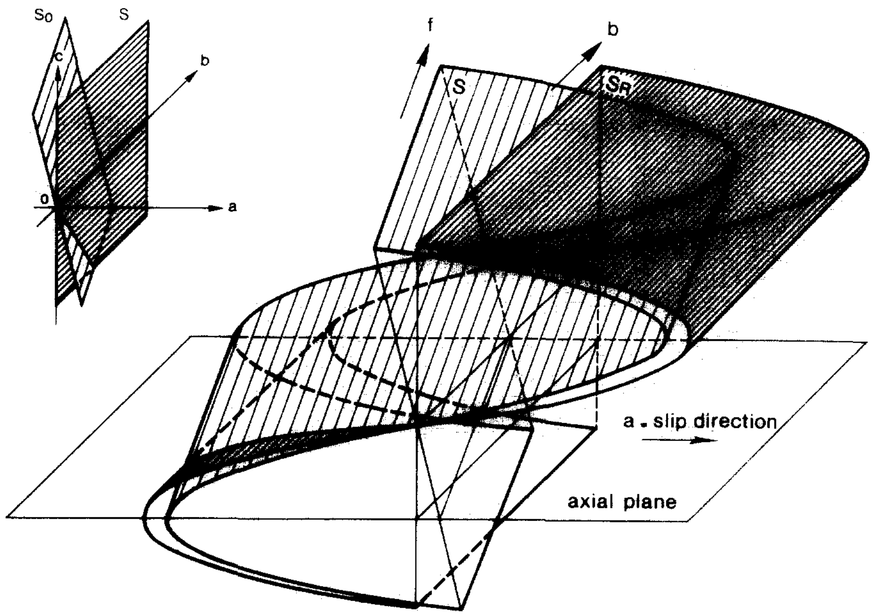


Fig. 1. Deformation of a plane by a similar fold phase. $a$ = slip direction, $c$ = pole of the axial plane, $b$ is perpendicular to $a$ and $c$. SR is the surface describing the applied folding motions, obtained after deformation of the vertical plane ($b$, $c$): the generatrix of this cylindrical surface is parallel to $b$. $S$ is the surface obtained after deformation of an oblique plane $S_0$: in this case, the generatrix of the cylindrical surface (i.e. the axis of the folded surface) is parallel to $f$, the intersection of $S_0$ with the axial plane.

model able to represent any interference of two or three similar fold phases.

## SIMILAR FOLDS AND INTERFERENCES

### *Similar folds*

Geometrically, a similar fold results from the application of a particular transformation $\Phi$, a similar fold phase, to a set of parallel planar layers (stratification $S_0$). $\Phi$ is entirely determined by two particular directions ($a$ the slip direction and $c$ the pole of the axial plane) and by a one-variable function $x = F(z)$ (profile function).

In 3D space ($0\, \boldsymbol{a}, \boldsymbol{b}, \boldsymbol{c}$), $\Phi$ transforms M ($x, y, z$) into M′ ($x', y', z'$) so that:

$$\overrightarrow{\mathrm{MM}'} = F(z) * \vec{a}. \qquad (1)$$

Then

$$\begin{aligned} x' &= x + F(z) \\ y' &= y \\ z' &= z. \end{aligned} \qquad (2)$$

The stratification $S_0$ may be variably oriented with respect to ($0\, \boldsymbol{a}, \boldsymbol{b}, \boldsymbol{c}$) (i.e. with respect to the characteristic orientations of $\Phi$).

The intersection of $S_0$ with the $\Phi$ axial plane will be designated $f$. If $f$ is parallel to the slip direction $a$, the fold phase has no effect since each stratification plane is transformed into itself. In all other cases, any particular plane $S_0$ is transformed by $\Phi$ into a cylindrical folded surface whose generatrix is parallel to $f$ (Fig. 1). $f$ is the axis of this folded surface. It should be noted that the $f$ axis, which is usually the most conspicuous fold parameter observed in the field depends on the original orientation of the stratification $S_0$ as well as on the $\Phi$ parameters. For this reason, axial directions are not used in the present work as a characteristic parameter of any particular similar fold phase.

A similar fold phase $\Phi$ transforms a stratification into a similar fold, i.e. into a set of parallel cylindrical surfaces. When all the points of the deformed planes are identical and cannot be distinguished from one another, one cannot define any slip direction by considering only the resulting fold. In fact, in this particular case, any direction belonging to the axial plane (except the $f$ axis) may be chosen as a slip direction (Fig. 2). However, this

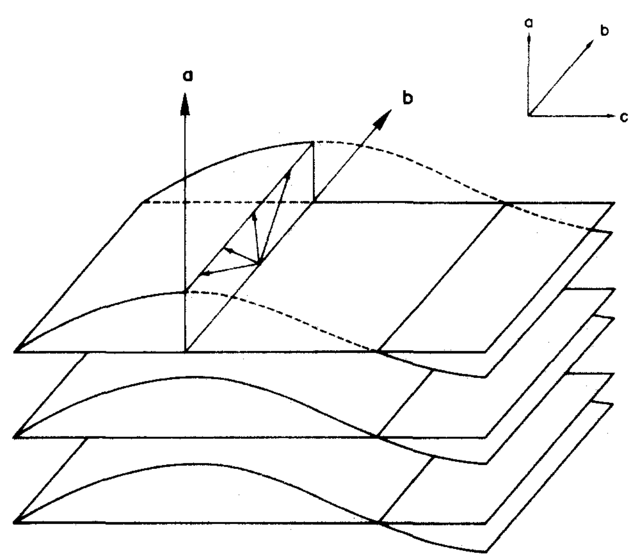


Fig. 2. Deformation of plane parallel layers by a similar fold phase. In this case, any direction of the axial plane, except $b$, may be chosen as a slip direction.

is generally no longer true when the original surfaces are not planes but already folded surfaces, i.e. when the result of the application of a similar fold phase is no longer a fold but a fold interference.

*Fold interferences*

A similar fold interference is the set of surfaces which results from the application of two or more similar fold phases to a stratification. Except in very particular cases, these surfaces are neither cylindrical nor parallel to one another. Moreover, when two similar fold phases are successively applied, the resulting interference pattern is dependent on the order in which they are applied (O'Driscoll 1964), except when they have the same axial plane (Thiessen & Means 1980) or the same slip direction (basin and dome interference, Ramsay 1967).

Let us consider two fold phases (Fig. 3):

$\Phi_1$ defined by an axial plane $S_1$, whose pole will be designated as $c_1$, and by a slip direction $a_1$;

$\Phi_2$ defined by an axial plane $S_2$, whose pole will be designated as $c_2$, and by a slip direction $a_2$.

The intersection of $S_1$ and $S_2$ will be designated as $p$.

$\Phi_1$ and $\Phi_2$ are applied successively to a stratification $S_0$, whose intersection with $S_1$ corresponds to a direction $f$. $f$ is the axis of the fold that would have resulted from the application of $\Phi_1$ to $S_0$. It may be variably oriented with respect to the slip direction $a_1$.

Following Ramsay (1967), Thiessen & Means (1980) have defined the various two-phase interference cases with the help of the following parameters (Fig. 3b).

Directions— $f$: axis of $\Phi_1$
$c_1$: pole of $S_1$
$d_1$: 'directrix' of $\Phi_1$, perpendicular to $f$ and $c_1$
$a_2$: slip direction of $\Phi_2$
$c_2$: pole of $S_2$
$b_2$: direction perpendicular to $a_2$ and $c_2$.

Angles— $\alpha$: $(f \wedge b_2)$
$\beta$: $(c_1 \wedge a_2)$
$\gamma$: $(f \wedge c_2)$
$\delta$: $(c_1 \wedge c_2)$.

Such parameters allow a correct descriptive study of two-phase fold interferences. However, these parameters are not fully independent of each other and they do not allow us to take into account *separately* the orientation of the stratification $S_0$ and the orientations of the transformation $(\Phi_1 + \Phi_2)$. For this reason, we define here new angles which allow us to consider the stratification $S_0$ and the transformation $(\Phi_1 + \Phi_2)$ as two different entities that may be variously tilted with respect to each other. The various interference cases will be discussed in terms of these new angular parameters. However, in order to avoid any possible misinterpretation, we consider, for each case, the equivalence of our criteria with those previously defined by Thiessen & Means, using angles $\alpha, \beta, \gamma$.

If we assume that $S_0$ is horizontal, we have to define two types of independent parameters in order to characterize the transformation itself $(\Phi_1 + \Phi_2)$ and its position

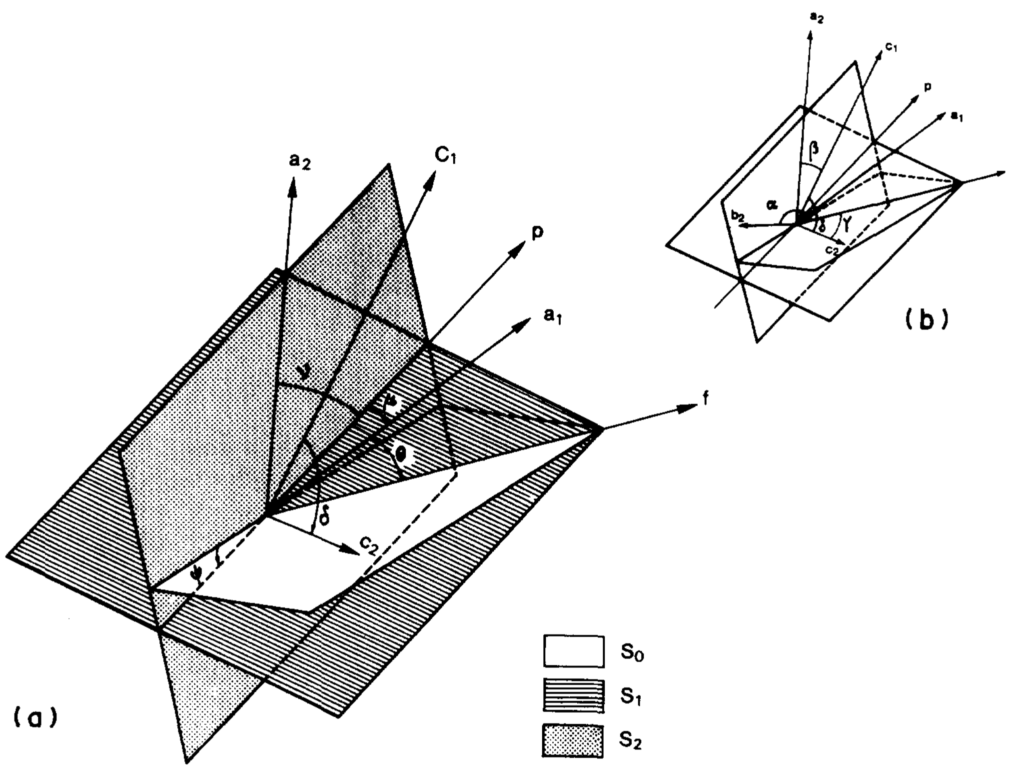


Fig. 3. Definition of the orientation parameters of two similar fold phases and of stratification. (a) Parameters used in the present paper. (b) Parameters defined by Thiessen & Means (1980).

in space (i.e. relative to $S_0$). The transformation ($\Phi_1 + \Phi_2$) only takes account of the orientation of the two fold phases relative to each other. This may be achieved by considering (i) the angle between the poles of the axial planes $S_1$ and $S_2$: $\delta = (c_1 \wedge c_2)$, and (ii) the angles between the slip directions and the intersection of $S_1$ and $S_2$: $\mu = (a_1 \wedge p)$, $\nu = (a_2 \wedge p)$.

In fact, since the first fold phase $\Phi_1$ is applied to planar surfaces $S_0$, any direction belonging to the axial plane—except the axis—may be chosen as a slip direction for $\Phi_1$. We may thus substitute $p$ for $a_1$ whenever the axis direction $f$ is not itself parallel to $p$. So, in general we do not need to take $\mu$ into consideration and ($\Phi_1 + \Phi_2$) is entirely defined by $\delta$ and $\nu$.

The position of ($\Phi_1 + \Phi_2$) with respect to $S_0$ may be characterized by two angles. We may choose for instance the angles $\theta$ and $\psi$ between $p$ and the intersections of $S_0$ with $S_1$ and $S_2$, respectively. Thiessen & Means (1980) have shown that the orientation of $S_0$ with respect to ($\Phi_1 + \Phi_2$) has an effect on the type of interference produced since it affects the value of the angle between $f$ and $c_2$ (their angle $\gamma$). Figure 3 shows that $(f \wedge c_2)$ depends on $\theta$ but not on $\psi$. Thus $\psi$ need not be taken into consideration.

In general, similar fold interferences may be studied with the help of three angles:

$\theta = (p \wedge f)$ which depends on the position of stratification $S_0$ with respect to ($\Phi_1 + \Phi_2$);

$\delta = (c_1 \wedge c_2)$ and $\nu = (a_2 \wedge p)$ which depend on the orientations of $\Phi_1$ and $\Phi_2$ relative to each other.

When $\theta = 0$, an additional angle $\mu = (a_1 \wedge p)$ must be considered.

The particular cases which have been defined by previous authors can now be examined.

*Type* 0 (Thiessen & Means 1980) may arise in the following situations. (a) Axial planes $S_1$ and $S_2$ are parallel to each other. This implies $\delta = 0$, corresponding to $\beta = \gamma = 90°$, $\alpha \neq 90°$ in Thiessen's & Means' classification. (b) Slip direction $a_2$ is parallel to $f$ which implies $\theta = 0$, $\nu = 0$. In Thiessen's & Means' classification, this case corresponds to $\alpha = \beta = \gamma = 90°$. (c) There is also the trivial case where slip direction $a_1$ is parallel to $S_0$ ($\theta = 0$, $\mu = 0$) so that there is no first fold at all.

*Coaxial interference* (Type 3 of Ramsay 1967, and Thiessen & Means 1980) occurs when the $f$ axis lies within the $S_2$ plane without being parallel to $a_1$ or to $a_2$. This implies $\theta = 0$. In order to exclude the Type 0 cases, we must add the condition: $\delta \neq 0$, $\mu \neq 0$, $\nu \neq 0$. The coaxial cases correspond, in Thiessen's & Means' classification, to the condition $\gamma = 90°$, which means that the $f$ axis is perpendicular to $c_2$ and thus parallel to $p$, and $\beta \neq 90°$, which means that these cases are not Type 0.

In all cases where $\delta \neq 0, \mu \neq 0, \nu \neq 0$, i.e. in all cases which are *not* Types 0 or 1 (basin and domes), one may find particular positions of $S_0$ which correspond to $\theta = 0$ ($\gamma = 90°$ in Thiessen's & Means' classification). This means that *in each case when the axial planes* $S_1$ *and* $S_2$ *and the slip directions* $a_1$ *and* $a_2$ *are, respectively, different from each other, there are particular positions of the stratification which exhibit coaxiality* (see Fig. 4).

*Basins and domes* (Type 1 interferences of Ramsay and Thiessen & Means) require that the $a_2$ slip direction lies within the $S_1$ plane. Since we do not consider the case when $S_1$ and $S_2$ planes are parallel to each other (Type 0), this condition means that $a_2$ is parallel to the intersection $p$ between $S_1$ and $S_2$. This implies $\nu = 0$. We have also $\theta \neq 0$ since the case $\nu = 0$, $\theta = 0$ corresponds to Type 0. For Thiessen & Means, basins and domes are produced when $\beta = 90°$ ($a_2$ parallel to $S_1$) and $\alpha \neq 0$ (since the condition $\beta = \gamma = 90°$ always corresponds to Type 0).

We have seen that one may choose any direction belonging to the axial plane $S_1$, except $f$, as a slip direction for $\Phi_1$, without changing the shape of the interference produced. Since $f$ is not parallel to $p$ in the case of basins and domes ($\theta \neq 0$), we may always consider that $p$ is the common slip direction for $\Phi_1$ and $\Phi_2$. Basins and domes are thus produced where the slip direction of the two fold phases may be considered as identical, if the orientations of $\Phi_1$ and $\Phi_2$ do not correspond to Type 0.

*A basin and dome interference pattern results from particular orientations of* $\Phi_1$ *and* $\Phi_2$ *with respect to each other and for any orientation of the stratification* except those ($\theta = 0$) which produce Type 0. It may be noted that the orientations of $\Phi_1$ and $\Phi_2$ which correspond to basin and dome can never produce a coaxial interference, even for particular values of $\theta$.

## A 3D SIMILAR FOLD INTERFERENCE MODEL

### *Choice of parameters*

The computer-aided model that we have produced allows a representation of any similar fold or any interference of two or more variably oriented similar fold phases. It is also able to represent faults. Stratification $S_0$ is defined as a variable number of horizontal layers whose thicknesses may be freely chosen. Different colours are assigned to the various layers (Figs. 7 and 8). Each fold phase $\Phi_n$ is characterized by its axial plane $S_n$ and its slip directions $a_n$, both of which may be chosen interactively, and by a profile function $F(z)$.

In a first version of the program achieved in 1985, $F(z)$ functions were sinusoids of variable amplitudes $A$ and wavelengths $L$. In a new version completed at the beginning of 1987, $F(z)$ may also be a 'handmade profile' defined by the user of the program with the help of a Benson digitizer. 'Stairlike' profiles can be used in order to model fault systems. An overall tilting of the model can also be imposed (Figs. 5 and 7).

Folds and interferences are represented through plane sections or block diagrams that may be oriented in any required direction. These are represented as visual images on a high-resolution colour screen whose plane

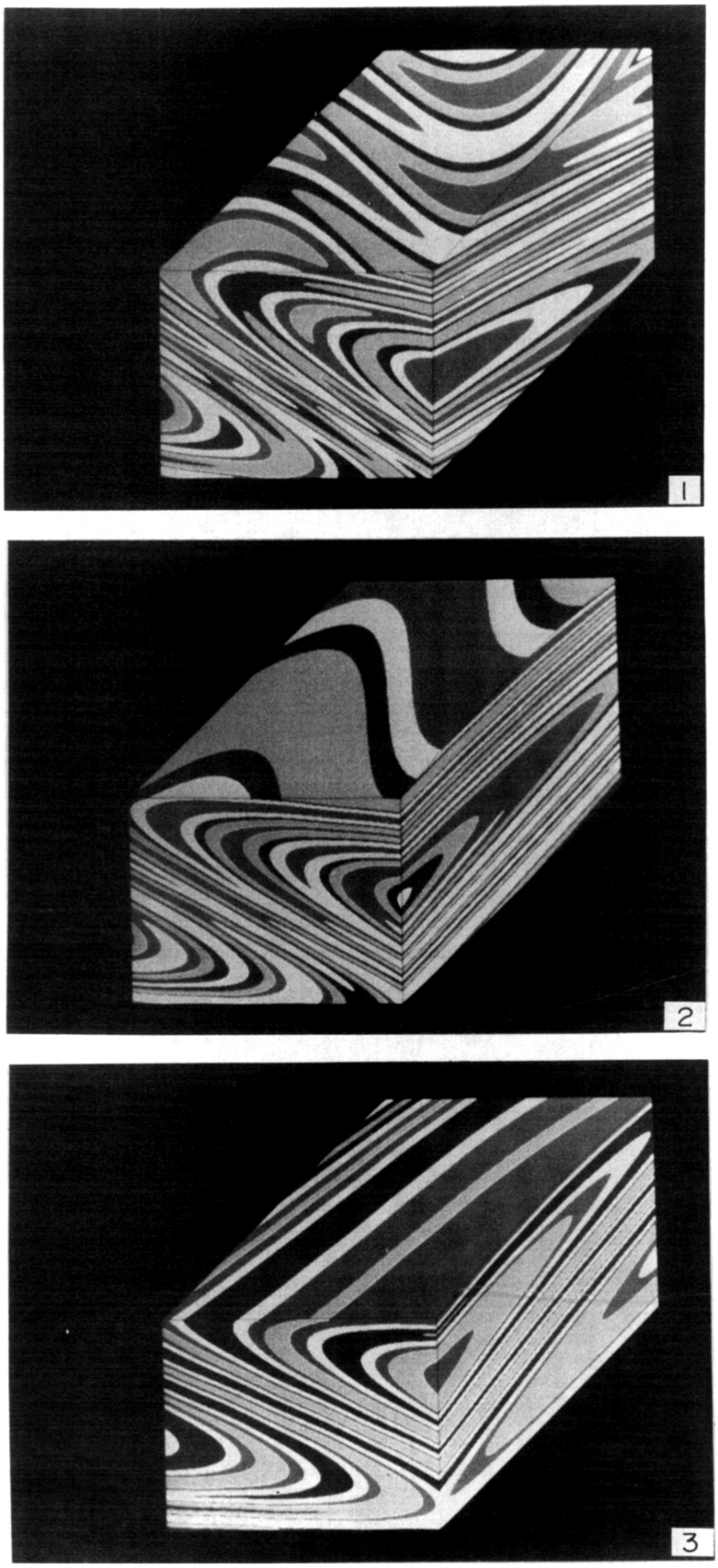


Fig. 4. Importance of the orientation of the stratification. The three models correspond to interferences of two similar fold phases whose orientations are the same with respect to each other ($\delta = 90°$, $\nu = 32°$) but are variable with respect to an originally horizontal stratification (1: $\theta = 30°$, 2: $\theta = 15°$, 3: $\theta = 0°$). Case number 3 corresponds to coaxiality.

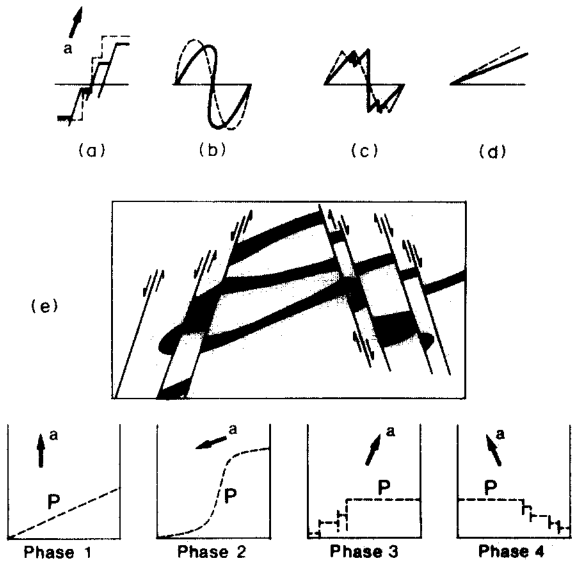


Fig. 5. Use of the various profile functions: (a) parallel faults, (b) sinusoidal fold profile, (c) handmade fold profile, (d) tilting. Application of four phases to achieve a faulted isoclinal fold pattern: (e) definition of the four phases. P and dashed lines = profile functions, $a$ = slip directions.

corresponds to the plane of the section or to the front plane of the block diagram.

Table 1 gives the list of the parameters that may be chosen interactively in the case of three fold phases with sinusoidal profiles.

*Building of a plane section*

The present model does not assume, as previously, that a stratification (or a fold or an interference) is a set of surfaces; it is now assumed to be a set of solid layers. It does not take into account the surfaces which separate the different layers, but only the individual points that are present inside each of them. Since we assign different colours to the different layers, we may consider that a stratification, a fold or an interference are all 3D sets of variously coloured individual points. The colour of each point indicates to which layer it belongs. A plane section through these objects may be considered as a 2D set of variously coloured points.

In order to build a plane section on a colour screen, we have to assign a particular colour to each of the screen pixels. Any particular pixel P results from the transformation of a particular point M belonging to $S_0$ by the similar fold phases concerned. To find out the colour of P, we thus have to identify the layer which contains M.

We have already seen that the displacement operated on a point M by a similar fold phase is:

$$\overline{MM'} = F(z) * \vec{a},$$

$\boldsymbol{a}$ being a unit vector parallel to the $\Phi$ slip direction and $z$ being measured perpendicularly to the $\Phi$ fold phase's axial plane. Conversely, if we wish to return to M, we must apply to M′ a displacement:

$$\overline{M'M} = -F(z) * \vec{a}.$$

This displacement corresponds to a similar fold phase $\Phi^{-1}$, whose orientations are the same as those of $\Phi$ but whose profile function is $-F(z)$.

Thus if $\Phi_1$ and $\Phi_2$ (and $\Phi_3$) are the two (or three) fold phases that we wish to introduce into the model and $F_1(z)$, $F_2(z)$, $F_3(z)$ their profile functions, P will be deduced from M through the application of $[\Phi_1 + \Phi_2\ (+\Phi_3)]$ and conversely M will be deduced from P through the application of $[(\Phi_3^{-1}) + \Phi_2^{-1} + \Phi_1^{-1}]$.

We have also seen that the application of a similar fold phase $\Phi$ to any point is easy, if we know the co-ordinates of the point concerned with respect to a co-ordinate system $(0\,\boldsymbol{a}, \boldsymbol{b}, \boldsymbol{c})$ fixed with respect to the pole of the axial plane and to the slip direction of $\Phi$. Thus before applying

Table 1. Choices available in the program

| | Choices | Values of the parameters (corresponding to Fig. 8a) | | | |
|---|---|---|---|---|---|
| Stratification | 128 lines,* 8 colours | lines 1–10 | | yellow | |
| | | lines 11–20 | | red | |
| | | lines 21–30 | | white | (repeated) |
| | | lines 31–40 | | green | |
| | | lines 41–128 | | blue | |
| Similar fold phases | Number of phases: 1–3 | Phase 1 | $S_1$ = 0/10°W | $A_1 = 1$ | $L_1/A_1 = 0.2$ |
| | $S$: orientations of axial planes | | $a_1$ = 090/10°W | | |
| | $a$: orientations of slip directions | Phase 2 | $S_2$ = 0/45°E | $A_2 = 0.5$ | $L_2/A_2 = 4$ |
| | $A$: amplitudes | | $a_2$ = 090/45°E | | |
| | $L/A$: wavelength/amplitude ratios | Phase 3 | $S_3$ = 090/90°N | $A_3 = 0.4$ | $L_3/A_3 = 6$ |
| | | | $a_3$ = 060/90°E | | |
| Block diagram | Dimension: 50–1000 | Dimension‡: 250 | | Orientation | $x = 35$ |
| | Orientation of the front plane | | | 090/90°S | $y = 180$ |
| | Origin (left bottom of the front plane): $x, y, z$† | | | | $z = 350$ |

* Each line is four pixels wide.
† The unit corresponds to one pixel.
‡ The parameter 'dimension' represents the number of pixels which correspond on the screen to the maximum length used in the definition of fold profiles, i.e. to the maximum value among $A_1$, $A_2$, $A_3$, $L_1$, $L_2$, $L_3$. In the present case $L_3$ is 250 pixels long. This allows a convenient choice of the scale of observation which is desired.

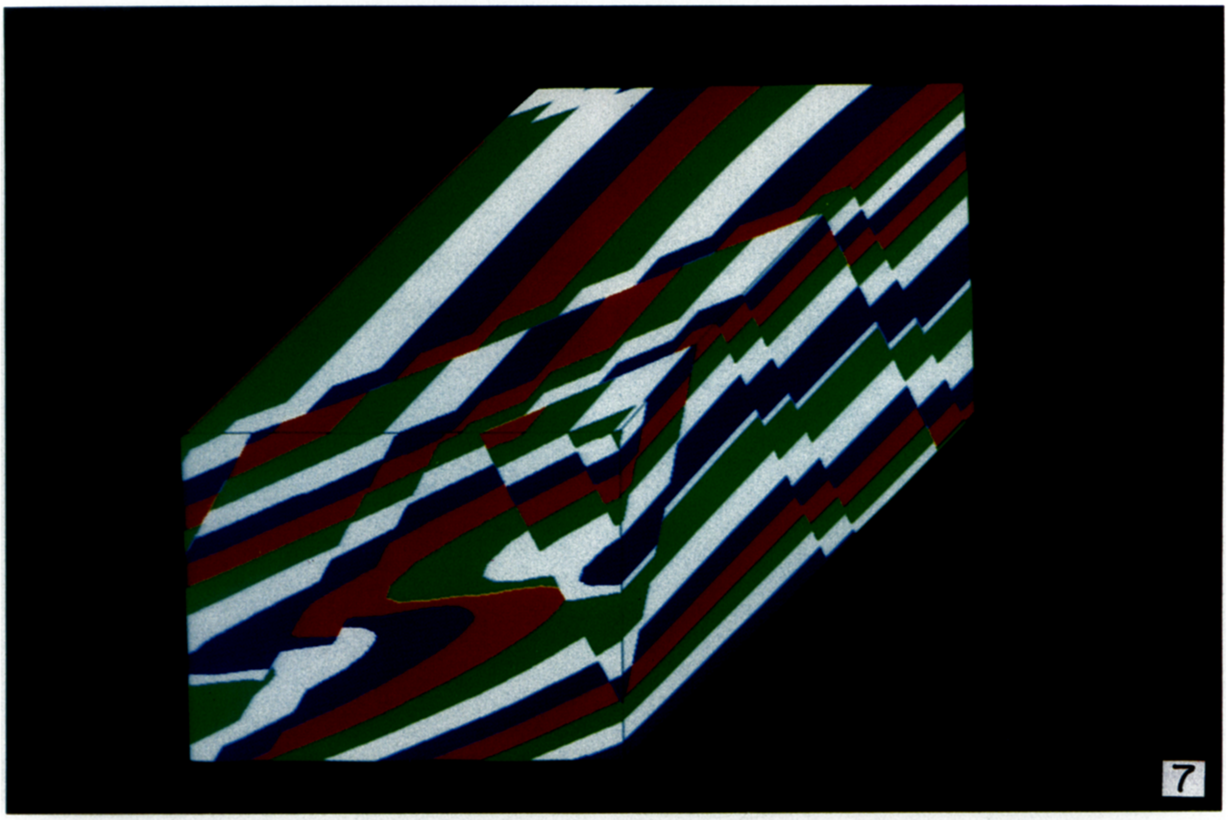

Fig. 7. Computer model derived from Fig. 5(e). The axial planes of the four phases have an orientation 060°/vertical.

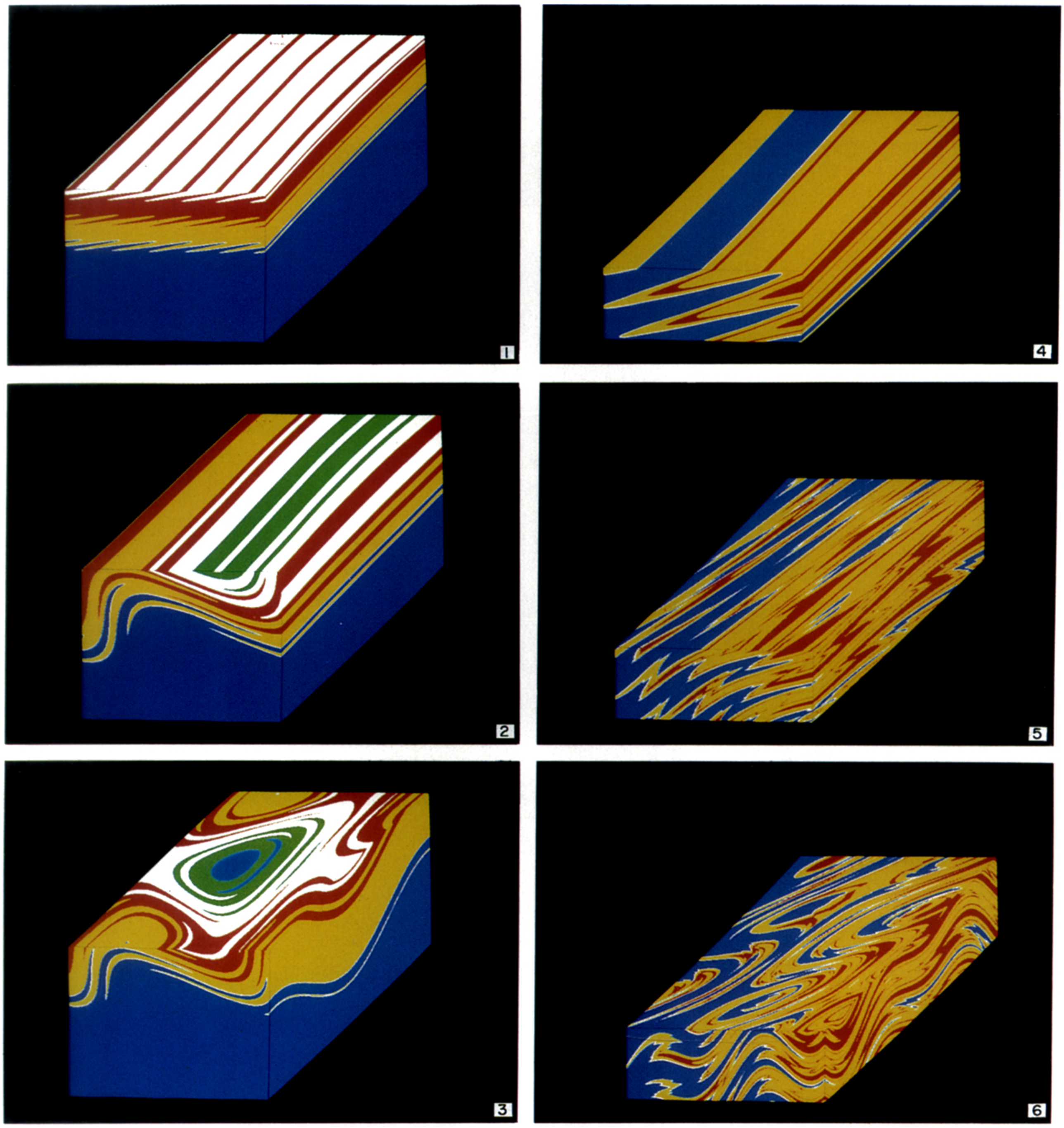


Fig. 8. (a) Frames (1)–(3). An example of three similar fold interferences, using sinusoidal profiles. (1): Phase 1: $S_1$ = 0/10°W, $a_1$ = 090/10°W, $L_1/A_1$ = 0.2. (2): Phases 1 + 2: $S_2$ = 0/45°E, $a_2$ = 090/45°E, $L_2/A_2$ = 4, $A_1/A_2$ = 2. (3): Phases 1–3: $S_3$ = 090°/vertical, $a_3$ = 060/90°E, $L_3/A_3$ = 6, $A_1/A_3$ = 2.5. (b) Frames (4)–(6). An example of six similar fold interferences using four sinusoidal profiles, one handmade profile and one tilting. (4): Phases 1 + 2. Phase 1: Tilting of 60°, $S_1$ = 0/10°W, $a_1$ = 060/90°S. Phase 2: Sinusoidal profile, $S_2$ = 0/18°W, $a_2$ = 090/18°W. (5): Phases 1–4. Phase 3: Handmade profile, $S_3$ = 030/45°W, $a_3$ = 120/45°W. Phase 4: Sinusoidal profile, $S_4$ = 035/45°E, $a_4$ = 125/45°E. Phase 5: Sinusoidal profile, $S_5$ = 050/90°S, $a_5$ = 110/90°S. Phase 6: Sinusoidal profile, $S_6$ = 090/90°S, $a_6$ = 0/90°W.

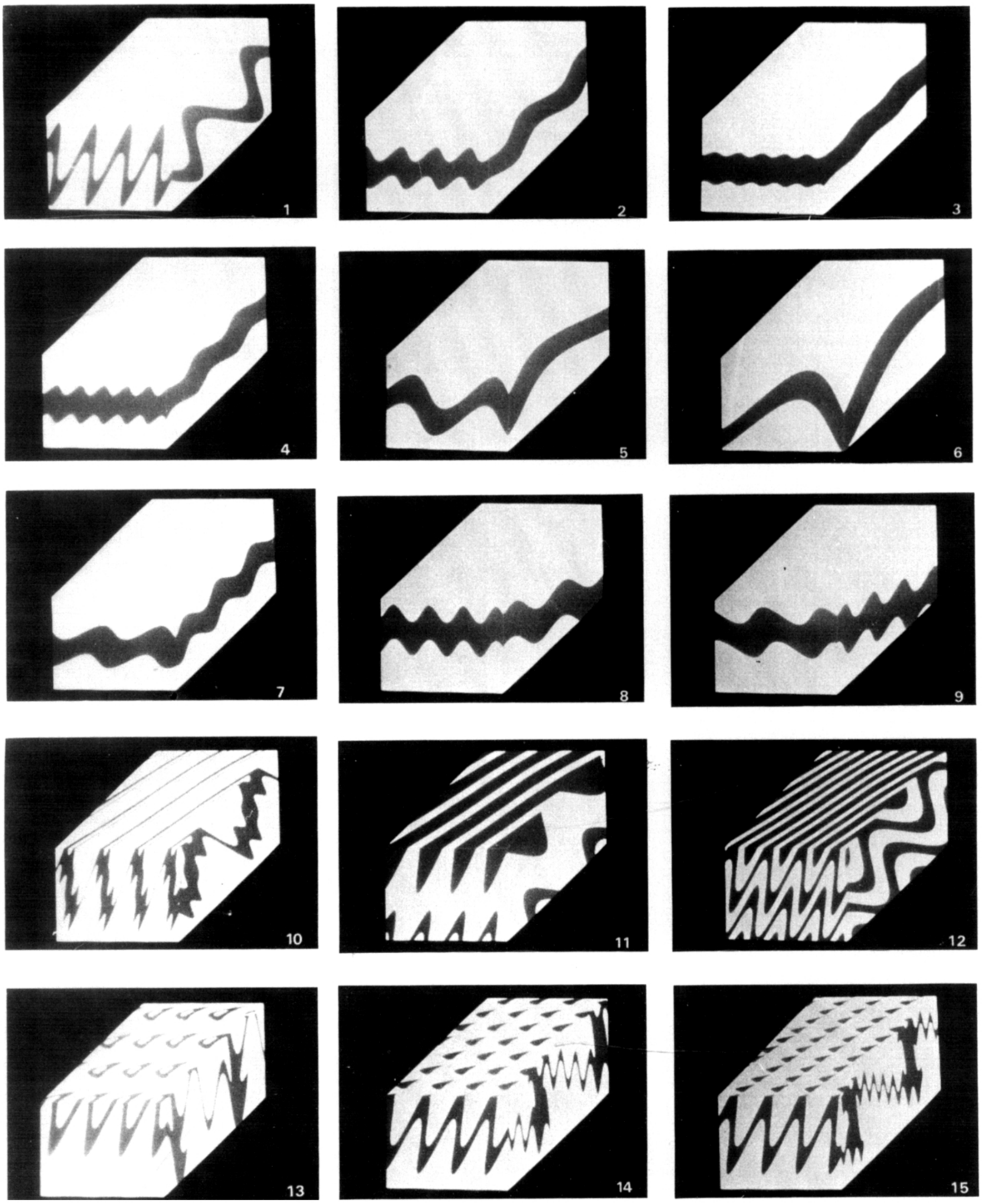


Fig. 9. Facilities of the multi-choice program of similar fold interferences. Block diagrams 320 × 250 pixels. Frames (1)–(12) One phase $\Phi_1$. (1)–(3) Influence of the shape of the sinusoidal profile: (1) $L_1/A_1 = 1$, (2) $L_1/A_1 = 4$, (3) $L_1/A_1 = 10$. (4)–(6) Influence of the relative dimension of the block diagram (compared to $A_1$): (4) Dimension 50, (5) Dimension 180, (6) Dimension 400. (7)–(9) Influence of the orientation of the block diagram: (7) front section 060/vertical, (8) front section 090/60°S, (9) front section 060/60°S. (10) Production of limb folds: addition of a phase $\Phi_2$ identical to $\Phi_1$, $L_1/A_1 = L_2/A_2 = 1$, $L_1/L_2 = 3$. (11) and (12) Influence of stratification $S$: (11) four layers of unequal thicknesses, (12) eight layers of equal thicknesses. (13)–(15) Influence of the relative wavelengths of two fold phases: $S_1$ = 030/75°W, $a_1$ = 120/75°W, $S_2$ = 090/90°S, $a_2$ = vertical, $L_1/A_1 = L_2/A_2 = 1$, (13) $L_1/L_2 = 0.5$, (14) $L_1/L_2 = 2$, (15) $L_1/L_2 = 3$.

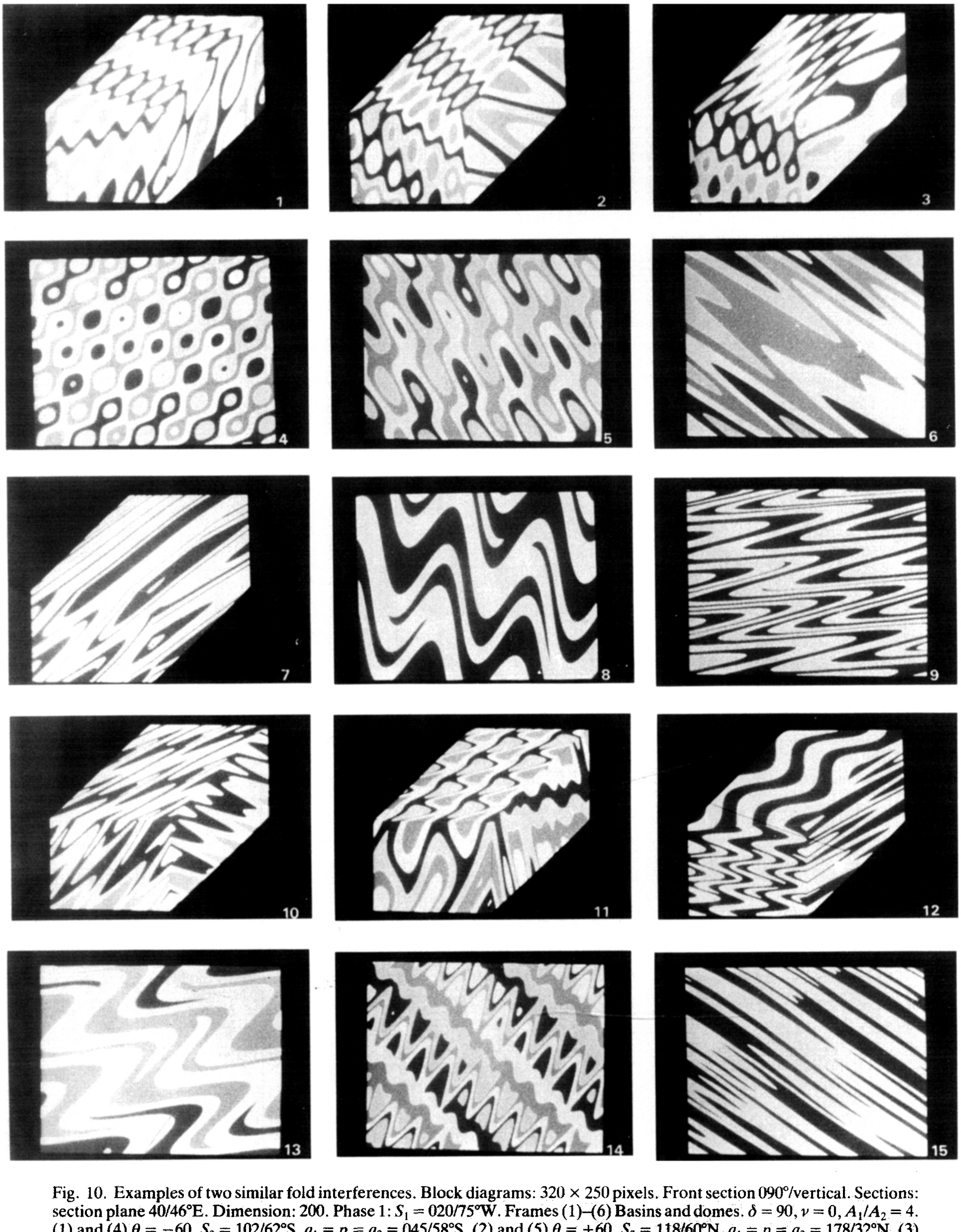


Fig. 10. Examples of two similar fold interferences. Block diagrams: 320 × 250 pixels. Front section 090°/vertical. Sections: section plane 40/46°E. Dimension: 200. Phase 1: $S_1$ = 020/75°W. Frames (1)–(6) Basins and domes. $\delta = 90$, $\nu = 0$, $A_1/A_2 = 4$. (1) and (4) $\theta = -60$, $S_2$ = 102/62°S, $a_1 = p = a_2$ = 045/58°S. (2) and (5) $\theta = +60$, $S_2$ = 118/60°N, $a_1 = p = a_2$ = 178/32°N. (3) (6) $\theta = +30$, $S_2$ = 134/32°N, $a_1 = p = a_2$ = 013/28°N. Frames (7)–(9) Coaxial interferences. $\theta = 0$, $A_1/A_2 = 0.5$, $a_1$ = 110/75°W. (7) and (8) $\delta = 30$, $\nu = 90$, $S_2$ = 020/45°W, $a_2$ = 110/45°W. (9) $\delta = 60$, $\nu = 90$, $S_2$ = 020/15°W, $a_2$ = 110/15°W. Frames (10)–(15) Type 2 interferences. $A_1/A_2 = 0.5$. (10) and (13) $\theta = 60$, $\delta = 30$, $\nu = 90$, $a_1 = p$ = 177/55°N, $S_2$ = 048/62°W, $a_2$ = 058/17°S. (11) and (14) $\theta = 90$, $\delta = 60$, $\nu = 10$, $a_1 = p$ = 127/75°N, $S_2$ = 085/80°N, $a_2$ = 107/65°W. (12) and (15) $\theta = 25$, $\delta = 75$, $\nu = 70$, $a_1 = p$ = 014/24°W, $S_2$ = 108/ 24°N, $a_2$ = 165/21°N.

each of the transformations $\Phi_3^{-1}$, $\Phi_2^{-1}$, $\Phi_1^{-1}$, it is necessary to perform the appropriate change of co-ordinate systems. In consequence, when two fold phases $\Phi_1$ and $\Phi_2$ are applied, we find the colour of any screen pixel P corresponding to a particular point M within $S_0$, through the following procedure:

(1) plotting the co-ordinates of P in a co-ordinate system related to $\Phi_2$;

(2) operating $\Phi_2^{-1}$;

(3) plotting the co-ordinates of the resulting point in a co-ordinate system related to $\Phi_1$;

(4) operating $\Phi_1^{-1}$;

(5) plotting the position of the resulting point M within the original stratification $S_0$;

(6) assigning to P the colour of the layer of $S_0$ which contains M.

The first five operations are easily achieved, making use of (3 × 3) matrices which take into account the orientations of $\Phi_1$ and $\Phi_2$ and of the plane section that we wish to see. Using this procedure the building of a section is achieved point by point and row by row.

*Building of a block diagram*

This step is easily implemented since we only perform at the present stage a representation using a parallel projection, which implies that sections located at the various distances from the front plane all have the same dimensions. On a screen of 512 × 640 pixels, we first build a front section of maximum dimension 250 × 320 pixels and then add extra lines and columns which correspond to the visible parts of extra sections located further and further away from the first front section. These extra sections are added step by step at the top and at the right-hand side of the front section in a 45° direction. This procedure is shown in Fig. 6.

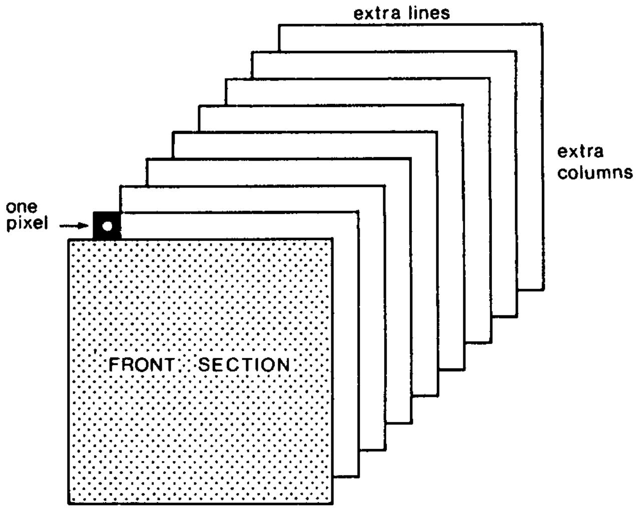


Fig. 6. Implementation of a block diagram.

*Representation through the running of a PASCAL program*

The computing procedure just explained is implemented in PASCAL under UNIX on the HP 9000 computer of the Ecole des Mines de Saint Etienne. Graphics output is achieved through a high-resolution LEXIDATA colour display, using the facilities of a LEXIDATA graphic memory.

Using these facilities, we are able to plot any section of a structure created by the interference of three similar fold phases, such as the one represented in Fig. 8(a), in an average time of 4 min. Figure 9 shows some of the facilities of the multichoice program for the representation of block diagrams.

## RESULTS

*Two similar fold interferences*

An atlas of interference patterns for sinusoidal fold profiles can be built up (Fig. 10).

The various parameters have been chosen as follows.

*Stratification* $S_0$. Four horizontal layers, each 32 lines thick.

$\Phi_1$ *orientations*. Fixed value of the axial plane: 020/75°W (which does not correspond to any particular case). The $\Phi_1$ slip direction is chosen parallel to $p$ and thus depends in each case on the orientation of $\Phi_2$. A change of the slip direction of the first phase has no consequence on the shape of the folds produced but only on their amplitude. Since the amplitude $A$ is an independent parameter which may be adjusted interactively, the choice of a particular slip direction $a_1$ within plane $S_1$ has no unexpected consequence on the shape of the resulting interference.

$\Phi_2$ *orientations*. These are chosen to fully explore the interference field by imposing proper successive values to $\theta, \delta, \nu$.

For each $(\theta, \delta, \nu)$ set, the values of the orientations of $p$, $a_2$ and $c_2$ are computed by means of a stereographic projection.

The shape of the fold profiles is fixed for both $\Phi_1$ and $\Phi_2$ by the ratio $L_1/A_1 = L_2/A_2 = 0.6$. The $L_1/L_2$ ratio is allowed for each $(\theta, \delta, \nu)$ to take the following five values: 4, 2, 1, 0.5, 0.25.

Visualization is performed on the LEXIDATA screen through block diagrams with a front plane of 320 × 250 pixels chosen with an orientation of 090°/vertical and/or through diagonal sections by a plane of chosen orientation 040/46°E the horizontal of the plane section being identical to the horizontal of the screen.

Figure 10 gives some examples of the results that have been obtained.

*Three similar fold interferences*

The variety of patterns that may result from three similar fold interferences with sinusoidal fold profiles is too great for systematic study. However the model allows us to build any given three fold interference that may be imagined. Results (e.g. Fig. 9) show that the model is able to produce patterns which closely resemble mapped interferences observed in the field.

*Multiply folded and faulted models*

In its present version, the program allows us to build models by operating up to 10 similar fold phases one after the other. For each of these phases, one can choose interactively the orientations (axial plane and slip direction), the profile (sinusoidal, stairlike, handmade, tilt profile) and the amplitude with respect to the other phases. We are thus able to provide a realistic representation of the geometry of multiply folded and faulted layers in all the cases when this geometry may be considered as the result of a combination of faults and similar folds. We introduce and adjust the various phases one after the other and control the results at each stage by comparing with the geometry of a hand specimen or outcrop pattern that we wish to reproduce. When all the parameters have been adjusted, the final model is produced in a few minutes. Figures 5 and 7 show the results obtained in the modelling of a multifaulted isoclinal fold, and Fig. 8(b) illustrates a six-phase similar fold interference using both sinusoidal and handmade profiles.

## DISCUSSION AND CONCLUSIONS

*Study of folds and interferences*

Our re-examination of two similar fold interferences has proved that some progress can be made in the description and interpretation of the corresponding patterns by allowing for:

(1) the position of the stratification with respect to the orientations of the interfering phases: coaxiality is achieved for particular orientations of $S_0$ which exist in all cases which are not basins and domes;

(2) variable fold profiles (sinusoids of variable wavelengths and amplitudes) and 'handmade' profiles that can reproduce the exact profile of folds observed in the field.

This versatile model is a great help in interference studies since it allows the swift construction of any similar fold interference and the display of the corresponding patterns. It allows systematic studies such as building up a two-phase fold interference atlas. Our results confirm those already reported by Thiessen & Means (1980) and by Thiessen (1986) and also extend them since we introduce systematic variations of the position of the stratification with respect to the orientations of the two fold phases and of the amplitudes of these two phases with respect to each other. However, the practical use of such an atlas is limited: nature shows similar folds profiles which are very varied and which often differ widely from sinusoids. Thus only a small part of the existing natural interferences of similar folds can be taken into account in a systematic way.

*Field modelling*

The use of computer graphics for the modelling of geological situations actually observed in the field is promising. Figure 11 shows a mapped natural interference pattern which compares well with examples in Fig. 8.

Our program in its present day version is able to produce a 3D model of multifolded and multifaulted terranes, in all cases where folds are 'similar' and where fault surfaces are planes. One model limitation is that bedding is assumed to be passive. This seems a reasonable assumption for similar folds generated in deep-seated terranes, but less so for folds generated under low


Fig. 11. Simplified geological map of the axial zone of Montagne Noire (Massif Central, France) from Demange (1979). Notice the strong topological similarities with the models shown in Fig. 8 frames (3) and (6).

confining pressure. We are planning to make further progress in the near future in the field of modelling concentric folds. We shall also aim to represent the intersection of 3D models such as the one which is already built, with an actual topography. This will allow us to produce synthetic geological maps that may be compared point by point with results from field mapping.

More generally, we aim to build a deterministic geometrical model from field data. Such a model would allow us to determine the shape and orientation of any layer at any point on the ground surface or underground, as well as the representation of the underground topography of any layer. Such field models could of course be checked and refined very easily by comparison of the results they give with all the orientation data collected in the field, as well as with other data such as geophysical results.

*Acknowledgements*—The present work results from a co-operation between the Geology and Computer Graphics teams of the Ecole des Mines de St Etienne. The study of similar fold interferences has been mainly the responsibility of M. Perrin and the PASCAL programming the responsibility of P. H. Oltra. We wish to thank E. Rommel for the achievement of 'handmade profiles', J. J. Motte and F. Avondo for the illustrations and G. Bronner, D. Ghazanfarpour, M. Beigbeder and B. Peroche for useful discussions and critical reviews.

## REFERENCES

Carey, S. W. 1954. The rheid concept in geotectonics. *J. geol. Soc. Aust.* **1**, 67–117.

Carey, S. W. 1962. Folding. *J. Alberta Soc. Petrol. Geol.* **10**, 95–144.

Charlesworth, H. A. K. & McLellan, G. C. 1986. Refold: a Fortran 77 program to construct model block diagrams of multiply folded rocks. *Comput. & Geosci.* **2**, 349–360.

Demange, M. 1979. Schéma structural de la partie orientale du massif de l'Agout (Montagne Noire). *Bull. Bur. Rech. géol. & Minières (Fr.)*, 2 *Ser.* **1**, 45–49.

Knopf, E. V. & Ingerson, E. 1938. Structural petrology. *Mem. geol. Soc. Am.* **6**.

O'Driscoll, E. S. 1962. Experimental patterns in superposed similar folding. *J. Alberta Soc. Petrol. Geol.* **10**, 145–167.

O'Driscoll, E. S. 1964. Interference patterns from inclined shear fold systems. *Can. Petrol. Geol.* **12**, 279–310.

Ramsay, J. G. 1962a. Interference patterns produced by the superposition of folds of "similar" type. *J. Geol.* **70**, 466–481.

Ramsay, J. G. 1962b. The geometry and mechanics of formation of similar type folds. *J. Geol.* **70**, 309–327.

Ramsay, J. G. 1967. *Folding and Fracturing of Rocks*. McGraw-Hill, New York.

Thiessen, R. L. & Means, W. D. 1980. Classification of fold interference patterns: a re-examination. *J. Struct. Geol.* **2**, 311–316.

Thiessen, R. 1986. Two-dimensional refold interference patterns. *J. Struct. Geol.* **8**, 563–573.

Turner, F. J. 1948. Mineralogical and structural evolution of metamorphic rocks. *Mem. geol. Soc. Am.* **30**.

Turner, F. J. & Weiss, L. E. 1963. *Structural Analysis of Metamorphic Tectonites*. McGraw-Hill, New York.

Weiss, L. E. 1959. Geometry of superposed folding. *Bull. geol. Soc. Am.* **70**, 91–106.

Whitten, 1959. A study of two directions of folding. *J. Geol.* **67**, 14–47.